ORIGINAL ARTICLE

Impact of Region of Interest Size on Semi-Quantification of Myocardial ^{99m}Tc-pyrophosphate Uptake in Suspected Transthyretin Cardiac Amyloidosis

Toshinori Saitou, RT[1)], Osamu Manabe, MD, PhD[2)], Atsushi Nagase, RT[1)], Hiroaki Toyama, RT[1)], Tamaki Kudo, RT[1)], Noriko Oyama-Manabe, MD, PhD[2)], and Tadao Aikawa, MD, PhD[2), 3), 4)]

Received: June 18, 2025 / Revised manuscript received: August 11, 2025 / Accepted: August 20, 2025
J-STAGE advance published: September 19, 2025
©The Japanese Society of Nuclear Cardiology 2025

Abstract

***Background*: This study aimed to evaluate the optimal region of interest (ROI) size of the heart-to-contralateral (H/CL) ratio on planar imaging for detecting myocardial technetium-99m pyrophosphate (PYP) uptake in patients with suspected transthyretin cardiac amyloidosis (ATTR-CA) and to assess the impact of ROI size on intra- and interobserver variability in the H/CL ratio.**

***Methods*: We retrospectively analyzed 90 consecutive patients who underwent PYP imaging for ATTR-CA evaluation after excluding 20 patients without myocardial PYP uptake on planar images (i.e., Grade 0). The H/CL ratio was measured using three ROI sizes (4.5 cm, 3 cm, and 2 cm). Receiver operating characteristic (ROC) analysis was used to evaluate the performance of each ROI size in detecting positive PYP single-photon emission computed tomography (SPECT). Intra- and inter-observer variability was assessed using intraclass correlation coefficients (ICCs).**

***Results*: Grade 2-3 myocardial PYP uptake on SPECT was observed in 41 (46%) patients. ROC analysis revealed no significant differences in the area under the curve among the various ROI sizes at 1 hour (0.68, 0.71, and 0.71 for the 4.5-, 3-, and 2-cm ROIs, respectively; *P*=0.44) or 3 hours (0.71, 0.72, and 0.72 for the 4.5-, 3-, and 2-cm ROIs, respectively; *P*=0.86). The largest ROI (4.5 cm) demonstrated the highest reproducibility, with excellent intra-observer (ICC=0.949) and inter-observer (ICC=0.906) agreement.**

***Conclusions*: The size of the ROI used to calculate the H/CL ratio did not significantly affect the detection of myocardial PYP uptake in patients with suspected ATTR-CA. Using a larger ROI size that covers the entire heart may improve the reproducibility of the H/CL ratio measurement.**

Keywords: ^{99m}Tc-pyrophosphate scintigraphy, Heart-to-contralateral lung ratio, Region of interest, Transthyretin cardiac amyloidosis
Ann Nucl Cardiol 2025; 11 (1): 33–38

Technetium-99m pyrophosphate (PYP) scintigraphy is widely used for the non-invasive evaluation of transthyretin cardiac amyloidosis (ATTR-CA). PYP planar imaging is generally evaluated using visual grading and the heart-to-contralateral lung uptake (H/CL) ratio (1, 2). A previous multicenter study revealed a high diagnostic accuracy of the H/CL ratio (≥1.5 at 1 hour or ≥1.3 at 3 hours after tracer injection) in detecting myocardial PYP uptake in patients with ATTR-CA, with sensitivity and specificity of approximately 90% (3). The H/CL ratio is also useful for differentiating ATTR-CA from light-chain cardiac amyloidosis (2). However, some studies have shown that the H/CL ratio is less accurate than visual scoring on planar images in detecting myocardial PYP uptake on single-photon emission computed tomography

DOI: 10.17996/anc.25-00005

1) Department of Radiology, Hokkaido Cardiovascular Hospital, Hokkaido, Japan
2) Department of Radiology, Jichi Medical University Saitama Medical Center, Saitama, Japan
3) Department of Cardiovascular Biology and Medicine, Juntendo University Graduate School of Medicine, Tokyo, Japan
4) Department of Cardiology, Hokkaido Cardiovascular Hospital, Hokkaido, Japan

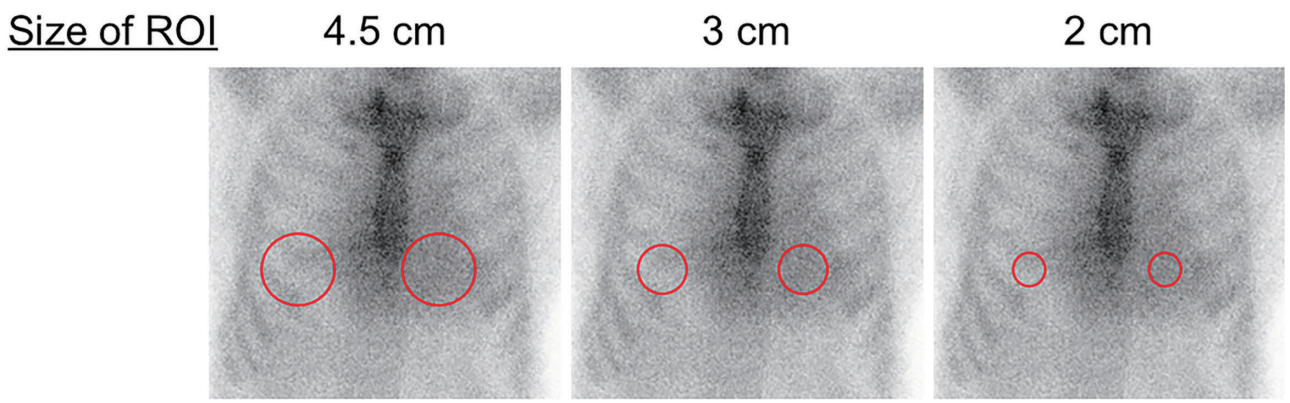

Figure 1 Examples of setting the ROI for measuring the H/CL ratio using an anterior planar image.
The ROI of the heart was set at its center by adjusting the ROI size for three types. The center of the heart was defined as the point midway between the sternum and the left end of the heart. The ROI of the contralateral lung field was set to avoid the right ventricle, vertebral bodies, and sternum.

(SPECT) (4–6). One reason for the lower specificity of the H/CL ratio is its susceptibility to blood pool and bone uptake (7, 8). Therefore, the recent American Society of Nuclear Cardiology (ASNC) expert consensus recommendations emphasize that ATTR-CA diagnosis cannot be made solely based on the H/CL ratio on PYP imaging (1).

Variation in the region of interest (ROI) used to calculate the H/CL ratio may also contribute to its low specificity in detecting myocardial PYP uptake. The ASNC expert consensus recommends maximizing the ROI over the heart without including the adjacent lungs (1). However, the lack of a standard heart ROI size may lead to variations in the H/CL ratio, particularly in patients with equivocal myocardial or blood pool PYP uptake. Therefore, this study aimed to evaluate the optimal ROI size of the H/CL ratio for detecting myocardial PYP uptake in patients with suspected ATTR-CA and to assess the impact of ROI size on intra- and interobserver variability in the H/CL ratio.

Materials and methods

Study population

The study cohort included consecutive patients who underwent PYP imaging for ATTR-CA evaluation at Hokkaido Cardiovascular Hospital, Japan between May 2020 and October 2020. The primary purpose of PYP imaging in this cohort was to assess ATTR-CA in patients with heart failure with preserved left ventricular ejection fraction (LVEF) or increased left ventricular mass index on echocardiography (5, 9, 10). The study protocol was approved by the Institutional Review Board of the Hokkaido Cardiovascular Hospital (IRB No. 2021-2). The requirement for written informed consent was waived owing to the retrospective nature of the study. Data on patient background and characteristics were extracted from electronic medical records.

PYP image data acquisition

PYP planar images in the anterior view were acquired for 5 minutes at 1 and 3 hours after the intravenous injection of 370-740 MBq of PYP (PDRadiopharma Inc., Tokyo, Japan) on a 256 × 256 matrix with a 1.33 zoom, followed by a SPECT scan of the thoracic region using a dual-head SPECT camera equipped with low-energy, high-resolution collimators (Infinia, GE Healthcare), as previously reported (5, 9). In SPECT, the matrix size was configured to 64 × 64 with a 360° rotation. PYP imaging was performed in accordance with the ASNC expert consensus recommendation (1).

PYP image data analysis

Myocardial PYP uptake on anterior planar and SPECT images was interpreted using visual scores (0 = no uptake; 1 = uptake less than the rib; 2 = uptake equal to the rib; 3 = uptake greater than the rib) (1). PYP imaging was considered positive when myocardial PYP uptake on SPECT at 3 hours after tracer injection was Grade 2 or 3 (1). The H/CL ratio on the anterior planar image was calculated by dividing the mean count of a circular ROI over the heart by the mean count of a ROI of the same size over the contralateral lung field. These ROIs were placed symmetrically and excluded the right ventricle, vertebral bodies, and sternum as much as possible (5, 9). The maximum ROI was set at 4.5 cm to ensure that it would not extend beyond the heart. The center position was kept the same, but the radius was adjusted. The H/CL ratio was measured using three ROI sizes (4.5, 3, and 2 cm) (Figure 1). To assess intra-operator repeatability, an experienced radiology technologist (T.S.) processed all image data twice, with an interval of 1 month. To assess inter-operator reproducibility, a second technologist (A. N.) analyzed the same datasets independently using the three ROI sizes in a blinded manner. Both T.S. and A.N. have more than 10 years of experience in nuclear medicine imaging. In this study population, 59

patients underwent computed tomography (CT) scans for clinical purposes. We generated fusion SPECT and CT images using a dedicated workstation (Xeleris 4DR, GE Healthcare) and software (Volumetrix MI, GE Healthcare) to assess myocardial PYP accumulation more accurately (5, 9–11). CT images were obtained before or after PYP imaging, with a mean interval of 182 days (interquartile range [IQR], 20–487 days) between examinations.

Statistical analysis

Continuous variables were expressed as medians with IQRs and compared using the Wilcoxon rank-sum test. Categorical variables were presented as numbers with percentages and compared using the Fisher's exact test. Paired data were compared using the Wilcoxon signed-rank test. A receiver operating characteristic (ROC) curve was plotted to estimate the area under the curve (AUC). ROC curves were compared using the chi-squared test. Inter-observer reproducibility and intra-observer repeatability were assessed using the intraclass correlation coefficient (ICC): ICC (1,1) was used for intra-observer repeatability based on a single-rater, absolute agreement, two-way mixed-effects model, and ICC (2,1) was used for inter-observer reproducibility based on a single-rater, absolute agreement, two-way random-effects model. The ICCs were categorized as follows: <0.50, poor correlation; 0.50–0.75, moderate correlation; 0.75–0.90, good correlation; and >0.90, excellent correlation. Statistical significance was defined as a P value <0.05. All statistical analyses were performed using JMP Pro 18.0.2 (SAS Institute Inc., Cary, NC, USA).

Results

Patient population

A total of 110 patients underwent ^{99m}Tc-PYP imaging. Of these patients, 20 with Grade 0 uptake on 3-hour planar images were excluded because the heart ROI could not be determined. Therefore, 90 patients (median age, 79 years [IQR, 73–86]) were included, most of whom (68%, $n=61$) were male. The median LVEF and left ventricular mass index were 56.6% (IQR, 47.9%–62.6%) and 108 (IQR, 99-122) g/m^2, respectively. Myocardial PYP uptake was observed on SPECT images in 41 patients (46%), five of whom were histologically diagnosed with ATTR-CA. Meanwhile, most patients did not undergo an endomyocardial biopsy owing to advanced age (≥ 80 years), a history of atrial fibrillation requiring anticoagulation, or the rapid spread of the COVID-19 pandemic during the study period, which precluded the diagnostic procedures involving pathological tissue analysis requiring hospitalization. No statistically significant differences in age, LVEF, and left ventricular posterior wall thickness were observed between patients with positive and negative PYP SPECT results. Compared with patients with negative PYP SPECT, those with positive PYP SPECT had a higher H/CL ratio for each ROI size on 1-hour and 3-hour planar images ($P<0.01$ for all; Table 1).

Discriminative performance of different ROI sizes of the H/CL ratio in detecting myocardial PYP uptake on SPECT

Figure 2 shows the results of the ROC analysis for detecting positive PYP SPECT results according to different ROI sizes. The AUC values for the 4.5-, 3-, and 2-cm ROIs on 1-hour planar images were 0.68, 0.71, and 0.71, respectively. These values did not differ significantly across ROI sizes ($P=0.44$). The AUC values for the 4.5-, 3-, and 2-cm ROIs on 3-hour planar images were 0.71, 0.72, and 0.72, respectively. These values also did not significantly differ across ROI sizes ($P=0.86$).

Intra-observer repeatability and inter-observer reproducibility of H/CL ratio measurements

Table 2 shows the intra-observer repeatability and inter-observer reproducibility of the H/CL ratio on 3-hour planar images. Intra-observer agreement was excellent for the 4.5-, 3-, and 2-cm ROIs (ICC=0.949, 0.934, and 0.901, respectively). Inter-observer agreement was excellent for the 4.5-cm ROI (ICC=0.906) and good for the 3- and 2-cm ROIs (ICC=0.848 and 0.773, respectively). Intra- and inter-observer agreements were better in patients with positive PYP SPECT than in those without, when the patients were stratified by SPECT positivity.

Discussion

In this study, we investigated whether differences in ROI sizes used to calculate the H/CL ratio on PYP planar imaging are related to the detection of myocardial PYP uptake on SPECT images. The discriminative performance of the H/CL ratio for detecting myocardial PYP uptake on SPECT images was not significantly different between the different ROI sizes on 1-hour and 3-hour planar images. Intra- and inter-observer agreements for calculating the H/CL ratio were excellent for a 4.5-cm ROI, suggesting that a larger ROI size may be better for reproducibly calculating the H/CL ratio.

Visual assessment of myocardial PYP uptake using the anterior planar images is inherently subjective and susceptible to intra- and inter-observer variability, whereas the H/CL ratio provides numerical values that enhance objectivity, thereby improving reproducibility across facilities and imaging protocols. Furthermore, the H/CL ratio enables evaluation based on a standardized threshold, making it increasingly important in research, clinical trials, and long-term patient monitoring. The H/CL ratio serves as a practical tool for tracking changes in myocardial uptake over time and assessing

Table 1 Baseline characteristics of patients with suspected ATTR cardiac amyloidosis

Characteristics	Negative PYP SPECT (n=49)*	Positive PYP SPECT (n=41)	P value
Age, years	77 (72–84)	82 (74–88)	0.066
Female	12 (24%)	17 (41%)	0.11
Body mass index, kg/m^2	24.4 (22.1–26.4)	24.8 (22.2–26.9)	0.71
Hypertension	31 (63%)	26 (63%)	1.00
Dyslipidemia	20 (41%)	18 (44%)	0.83
Diabetes	16 (33%)	10 (24%)	0.49
Coronary artery disease	13 (27%)	11 (27%)	1.00
Prior myocardial infarction	3 (6%)	4 (10%)	0.70
Permanent pacemaker	7 (14%)	3 (7%)	0.34
Atrial fibrillation	30 (61%)	18 (44%)	0.14
Low ECG voltage †	9 (18%)	12 (29%)	0.32
Laboratory data			
NT-proBNP, pg/mL (n=84)	1,482 (282–4,014)	889 (237–2,240)	0.20
Creatinine, mg/dL	1.03 (0.82–1.54)	0.96 (0.70–1.19)	0.10
Estimated glomerular filtration rate, mL/min/1.73 m^2	49.5 (34.3–67.4)	51.3 (37.4–70.6)	0.44
Echocardiography data			
LV ejection fraction, %	56.5 (42.1–62.4)	57.0 (49.9–63.0)	0.43
LV mass index, g/m^2	108 (100–118)	109 (97–127)	0.84
LV interventricular septal thickness, mm	10.6 (9.5–11.6)	10.5 (9.4–11.6)	0.84
LV posterior wall thickness, mm	10.2 (9.5–10.9)	10.3 (9.1–11.3)	0.95
H/CL ratio of PYP planar imaging			
ROI size of 1-hour anterior planar images			
4.5 cm	1.31 (1.22–1.39)	1.38 (1.28–1.57)	0.003
3 cm	1.33 (1.27–1.43)	1.47 (1.34–1.66)	<0.001
2 cm	1.35 (1.29–1.44)	1.50 (1.36–1.69)	<0.001
ROI size of 3-hour anterior planar images			
4.5 cm	1.24 (1.19–1.32)	1.35 (1.24–1.49)	<0.001
3 cm	1.29 (1.23–1.35)	1.40 (1.30–1.56)	<0.001
2 cm	1.32 (1.20–1.38)	1.44 (1.33–1.60)	<0.001

* Patients with Grade 0 uptake on 3-hour planar images (n = 20) were excluded because the heart ROI could not be determined.
† Low ECG voltage was defined as QRS amplitude ≤0.5 mV in all limb leads or ≤1 mV in all precordial leads.
Data are presented as the median (interquartile range) or n (%).

treatment efficacy or disease progression. This method can be easily implemented using planar imaging, without requiring advanced image processing or reconstruction techniques.

Guidelines recommend that the ROI for calculating the H/CL ratio should be maximized over the heart without including the adjacent lungs (1). This study confirmed that the ROI size used to calculate the H/CL ratio did not affect the detection of myocardial PYP uptake on SPECT images when the ROI was less than 4.5 cm. Previous studies have shown the excellent reproducibility of H/CL ratio measurements (12, 13). However, in the present study, the inter-observer agreement of the H/CL ratio was decreased when a smaller ROI size was used. This is likely due to the greater influence of rib-induced PYP uptake as ROI size decreases (14).

In this study, the H/CL ratio in the SPECT-positive group were relatively low compared to those in other studies (6, 15), particularly when the ROI size was large and the imaging time was 1 hour. Blood pool radioactivity is higher in 1-hour planar images than in 3-hour planar images (5) because PYP is excreted in urine after intravenous injection. Although the planar image was acquired with the sternum and vertebral bodies aligned as much as possible, using a large ROI to calculate the H/CL ratio may include blood pool uptake in the contralateral lung field (e.g., the right atrium), which leads to lower H/CL ratios.

This study has several limitations. First, SPECT imaging is commonly used as a reference standard for evaluating myocardial PYP uptake; however, it does not directly reflect

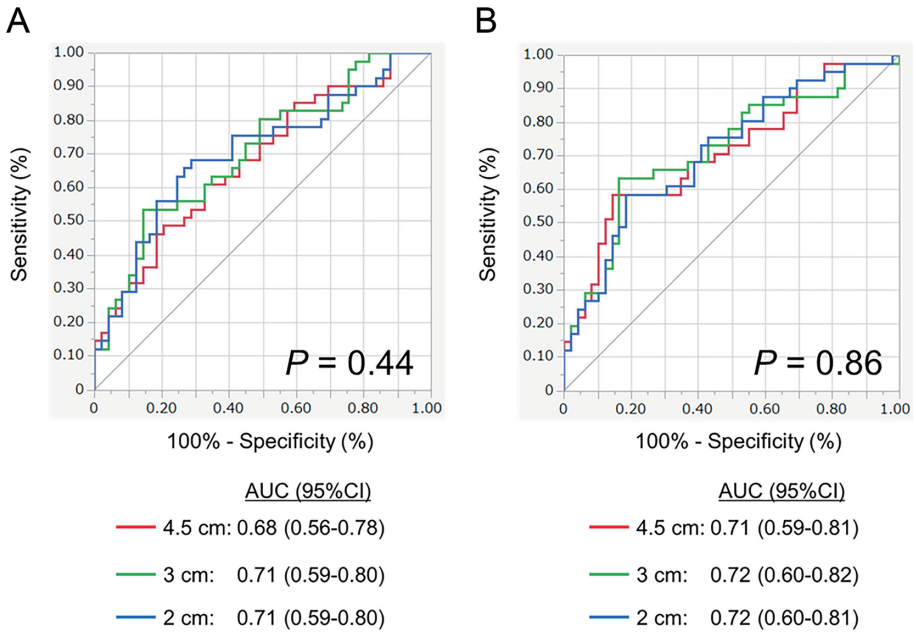

Figure 2 Receiver-operating characteristic curves with varying ROI sizes for detecting positive ^{99m}Tc-pyrophosphate SPECT results.
A: Comparison of AUC based on differences in ROI size for the H/CL ratio at 1 hour.
B: Comparison of AUC based on differences in ROI size for the H/CL ratio at 3 hours.
AUC, area under the curve; CI, confidence interval.

Table 2 Intra- and inter-observer agreements for the H/CL ratio at 3 hours after PYP injection

	ROI size	ICC (1,1) for intra-observer agreement	ICC (2,1) for inter-observer agreement
Overall (*n*=90)	4.5 cm	0.949	0.906
	3 cm	0.934	0.848
	2 cm	0.901	0.773
Positive SPECT (*n*= 41)	4.5 cm	0.979	0.920
	3 cm	0.977	0.865
	2 cm	0.957	0.784
Negative SPECT (*n*= 49)*	4.5 cm	0.810	0.787
	3 cm	0.764	0.715
	2 cm	0.713	0.634

*Patients with Grade 0 uptake on 3-hour planar images (*n*=20) were excluded because the heart ROI could not be determined.
ICC, intraclass correlation coefficients; H/CL, heart-to-contralateral lung uptake; ROI, region of interest

amyloid deposition confirmed by histopathology. Therefore, this study only evaluated the ability of the H/CL ratio to detect myocardial PYP uptake on SPECT imaging. Second, individual variations in heart size and anatomical structure may influence the appropriateness of ROI size and location for the H/CL ratio. In smaller patients, larger ROIs may encompass the lung and sternum, affecting detection accuracy. Therefore, future studies should verify the appropriateness and reproducibility of individualized ROI placement.

In conclusion, the size of the ROI used to calculate the H/CL ratio did not significantly affect the detection of myocardial PYP uptake in patients with suspected ATTR-CA. Using a larger ROI size covering the heart may improve the reproducibility of the H/CL ratio measurement.

Acknowledgments

None.

Sources of funding

This work was supported in part by Daiwa Securities Foundation (to Dr. Aikawa), Kanzawa Medical Research Foundation (to Dr. Aikawa), Fukuda Foundation for Medical Technology (to Dr. Aikawa), and Takeda Science Foundation (to Dr. Aikawa).

Conflicts of interest

Dr. Noriko Oyama-Manabe received payments for lectures from Bayer Healthcare, GE Healthcare Pharma, and Canon Medical Systems. The authors declare no conflicts of interest.

Reprint requests and correspondence:
Tadao Aikawa, MD, PhD, FACC, FESC
Department of Cardiovascular Biology and Medicine, Juntendo University Graduate School of Medicine, 2-1-1 Hongo, Bunkyo-ku, Tokyo 113-8421, Japan
E-mail: tadao.aikawa@juntendo.ac.jp

References

1. Dorbala S, Ando Y, Bokhari S, et al. ASNC/AHA/ASE/EANM/HFSA/ISA/SCMR/SNMMI expert consensus recommendations for multimodality imaging in cardiac amyloidosis: Part 1 of 2-evidence base and standardized methods of imaging. Circ Cardiovasc Imaging 2021; 14: e000029.
2. Bokhari S, Castaño A, Pozniakoff T, Deslisle S, Latif F, Maurer MS. ^{99m}Tc-pyrophosphate scintigraphy for differentiating light-chain cardiac amyloidosis from the transthyretin-related familial and senile cardiac amyloidoses. Circ Cardiovasc Imaging 2013; 6: 195–201.
3. Castano A, Haq M, Narotsky DL, et al. Multicenter study of planar technetium 99m pyrophosphate cardiac imaging: predicting survival for patients with ATTR cardiac amyloidosis. JAMA Cardiol 2016; 1: 880–9.
4. Asif T, Gomez J, Singh V, Doukky R, Nedeltcheva A, Malhotra S. Comparison of planar with tomographic pyrophosphate scintigraphy for transthyretin cardiac amyloidosis: Perils and pitfalls. J Nucl Cardiol 2021; 28: 104–11.
5. Saitou T, Aikawa T, Manabe O, Nagase A, Kudo T, Oyama-Manabe N. Comparison of 1-h with 3-h planar ^{99m}Tc-pyrophosphate scintigraphy in patients with suspected transthyretin cardiac amyloidosis using SPECT as a reference standard. Ann Nucl Med 2023; 37: 99–107.
6. Masri A, Bukhari S, Ahmad S, et al. Efficient 1-hour technetium-99 m pyrophosphate imaging protocol for the diagnosis of transthyretin cardiac amyloidosis. Circ Cardiovasc Imaging 2020; 13: e010249.
7. Hanna M, Ruberg FL, Maurer MS, et al. Cardiac scintigraphy with technetium-99m-labeled bone-seeking tracers for suspected amyloidosis: JACC review topic of the week. J Am Coll Cardiol 2020; 75: 2851–62.
8. Sperry BW, Burgett E, Bybee KA, et al. Technetium pyrophosphate nuclear scintigraphy for cardiac amyloidosis: Imaging at 1 vs 3 hours and planar vs SPECT/CT. J Nucl Cardiol 2020; 27: 1802–7.
9. Saitou T, Aikawa T, Manabe O, et al. Lateral planar imaging of ^{99m}Tc-pyrophosphate scintigraphy in patients with suspected transthyretin cardiac amyloidosis. Ann Nucl Cardiol 2024; 10: 29–37.
10. Ajima T, Aikawa T, Saitou T, et al. Prognostic value of ^{99m}Tc-pyrophosphate uptake in patients with suspected transthyretin cardiac amyloidosis. J Nucl Cardiol 2025. DOI: 10.1016/j.nuclcard.2025.102452
11. Kudo T, Kuji I, Nakajima K, et al. Nuclear medicine imaging for the diagnosis of ATTR cardiac amyloidosis: Report of Japanese Society of Nuclear Cardiology working group. Ann Nucl Cardiol 2025. DOI: 10.17996/anc.25-001
12. Singh V, Cuddy S, Kijewski MF, et al. Inter-observer reproducibility and intra-observer repeatability in ^{99m}Tc-pyrophosphate scan interpretation for diagnosis of transthyretin cardiac amyloidosis. J Nucl Cardiol 2022; 29: 440–6.
13. Ren C, Ren J, Tian Z, et al. Assessment of cardiac amyloidosis with ^{99m}Tc-pyrophosphate (PYP) quantitative SPECT. EJNMMI Phys 2021; 8: 3.
14. Onishi H, Sakai T, Shiromoto O, Amijima H. Validation of optimum ROI size for ^{123}I-FP-CIT SPECT imaging using a 3D mathematical cylinder phantom. Asia Ocean J Nucl Med Biol 2018; 6: 139–48.
15. Pandey S, Teruya S, Rodriguez C, et al. Diagnostic performance characteristics of planar quantitative and semi-quantitative parameters of Tc^{99m} pyrophosphate (PYP) imaging for diagnosis of transthyretin (ATTR) cardiac amyloidosis: the SCAN-MP study. J Nucl Cardiol 2023; 30: 1414–9.